Military Technical College
Kobry El-Kobbah,
Cairo, Egypt

17th International Conference on Applied Mechanics and Mechanical Engineering

ACTIVE VEHICLE SAFETY USING INTEGRATED CONTROL OF BODY ROLL AND DIRECT YAW MOMENT

A. Elhefnawy*, A. M. Sharaf*, H. M. Ragheb* and S. M. Hegazy*

ABSTRACT

This paper presents an integrated active roll control (ARC) and direct yaw control (DYC) system to improve both the rollover and cornering stability of the vehicle. The presented controller is developed based upon a combination of feedback and feedforward fuzzy logic control for roll control, and a fuzzy logic control for yaw rate.

A full vehicle model is used to describe and simulate the vehicle dynamics. Additionally, a yaw- roll plane model is introduced to compare and therefor control the yaw rate, the side slip angle and the roll angle of the vehicle body. Five input variables are considered by the three controllers namely; the vehicle foreword speed, the steering wheel angle, the roll angle, the yaw rate and the side slip angle of the vehicle body. The control action of the direct yaw control DYC and the active roll control ARC both are carried out by generating a differential braking across the front wheels. The numerical modeling is carried out through the MATLAB / SIMULINK environment which suits the control and optimization process.

Different simulation results are carried out by considering standard test maneuvers with different speeds such as J-turn, fishhook, and the lane change. The simulation results are compared during four cases namely; the uncontrolled system, the ARC controller only, the DYC controller only and the integrated ARC and DYC controllers. The results show a substantial improvement of the vehicle stability in term of vehicle lateral acceleration, side slip angle, the yaw rate and the roll angle for the developed integrated ARC and DYC controllers compared to that of the individual controller or the uncontrolled system. The main advantage of the proposed controller that it is relies on one actuation which is the differential braking.

KEY WORDS

Active roll control, direct yaw control, integrated control, fuzzy logic control

* Egyptian Armed Force.

NOMENCLATURES

a,b	Locationof theoriginofvehicleframeofreference from front and rear axle [m]
$C_{f,r}$	Damping coefficient of front/rear suspension [N.s/m]
$C_{\alpha f,\alpha r}$	Cornering stiffness of front, rear tires [N/rad]
F_{Xi}, F_{Yi}, F_{Zi}	Tire forces expressed at vehicle frame of reference [N]
F_{xi}, F_{yi}, F_{zi}	Tire forces expressed at wheel coordinate systems [N]
g	Gravitational acceleration [m/s^2]
I_{xx}, I_{yy}, I_{zz}	Mass moment of inertia of the vehicle sprung mass [Kg.m^2]
I_{xy}, I_{yz}, I_{zx}	Mass product moment of inertia of the vehicle sprung mass [Kg.m^2]
I_{wi}	Mass moment of inertia of wheels [Kg.m^2]
$K_{f,r}$	Stiffness coefficient of front/rear suspension spring [N/m]
L	Wheelbase (distance between front and rear axle) [m]
M_{B_i}	Braking moment applied to each wheel [N.m]
M_{D_i}	Driving moment applied at each wheel hub [N.m]
M_s	Sprung mass of the vehicle [Kg]
M_t	Total mass of the vehicle [Kg]
M_{U_i}	Resisting moment applied at each wheel hub [N.m]
M_{wi}	Unsprung mass at each wheel [Kg]
M_X, M_Y, M_Z	Net moments affecting the vehicle body [N.m]
p,q,r	Rotational velocities (roll, pitch and yaw) [rad/s]
$\dot{p},\dot{q},\dot{r}$	Rotational acceleration (roll, pitch and yaw) [rad/s^2]
r_{di}	Dynamic rolling radius of each wheel [m]
t_{rf}, t_{rr}	Wheel track at front and rear axle [m]
U,V,W	Translational velocities (forward, lateral and vertical) expressed at local frame of reference [m/s]
$\dot{U},\dot{V},\dot{W}$	Translational acceleration (forward, lateral and vertical) expressed at local frame of reference [m/s^2]
$Z_{bi}, \dot{Z}_{bi}$	Vertical velocities and acceleration at corners [m/s], [m/s^2]
$Z_{wi}, \dot{Z}_{wi}, \ddot{Z}_{wi}$	Wheel hub vertical position, velocity and acceleration [m], [m/s], [m/s^2]
ϕ,θ,ψ	Sprung mass angular displacement (roll, pitch and yaw) [rad]
$\omega_i, \dot{\omega}_i$	Wheel angular speed and acceleration [rad/s], [rad/s^2]

INTRODUCTION

Over the years, improving safety of ground vehicles during cornering with excessive speed, obstacle avoidance and severe lane change maneuvers has gained a lot of interest by the researchers worldwide. It is widely known that, vehicle safety is strongly related to both yaw and roll angular rotations of the vehicle body about its vertical and longitudinal axes respectively. With the advent of numerical control systems employing advanced optimization techniques, several safety systems have been introduced. For instance, *Electronic Stability Control* systems (ESC) have been originally introduced to stabilize the yaw motion and to prevent over or under steering accidents of modern road vehicles [1-5]. On the other hand, according to the control action, several active rollover prevention systems were proposed such as differential-braking [6-12], active front wheel steering [13], anti-roll bars [14, 15] and active suspension [16, 17] or an integration of different actuators [18-21]. The majority of approaches quantifies the rollover threat by an appropriate index and switches the control authority to a roll stabilizing controller when indicated. To mitigate rollover without affecting the yaw rate, the vehicle is countered-steer into the negative roll angle equilibrium during cornering [22].

The recent demands further imply integrating the aforementioned controllers, particular there is a mutual effect between the yaw and roll motions of the vehicle body. A yaw stabilizing control action, such as braking the outside turn front wheel as typically performed by ESC systems generates a yaw torque that counteracts the oversteering, increasing the radius of curvature, decreasing the lateral acceleration, and thus mitigating potential rollover threat as well. In addition, the lateral acceleration is reduced via the decreasing longitudinal velocity. The braking further limits the lateral tire force of that wheel, which is favorable in terms of rollover prevention. However, the braking action commanded by a yaw stabilizing control system might not be sufficient to prevent rollover. On the other hand, an increased braking action that successfully prevents rollover might be too aggressive in terms of yaw and destabilize the yaw motion. Furthermore, it is not possible to reduce the rollover threat by reallocation of tire forces without changing the yaw rate or vehicle speed [22]. Moreover, in addition to a braking of the outside turn front wheel, rollover can be effectively mitigated by braking all wheels. Taking advantage from the friction circle, lateral tire forces can be minimized by maximized longitudinal forces, that is, full brake application. This problem can be illustrated by discussing an oversteering scenario, considering differential braking for actuation, four different maneuvers with different speeds used for this purpose.

Based upon a combination of feedback and feedforward fuzzy logic control for roll control, and a fuzzy logic control for yaw rate, this paper presents an integrated active roll control (ARC) and direct yaw control (DYC) system to improve both the rollover and cornering stability of the vehicle. A 14-DOF nonlinear vehicle model with nonlinear tire model characteristics are described briefly then extract the reference model of integrated control system. The proposed integrated controller is designed based on model predictive control theory. Several numerical simulation are carried out to depict the response of the vehicle during different standard test maneuvers such as single and double lane change maneuver, J-turn maneuver and fishhook-turn maneuver.

MODEL DESCRIPTION

The presented work is based on a comprehensive 14 DOF full vehicle model which was developed and published by sharaf [23]. This model is further validated with an acceptable level of accuracy against the well know commercial packages such as highly complex models created in Adams-Car and medium sophisticated models created in CarSim. The model is less complex, yet adequate to represent vehicle dynamics accurately such that, it is possible to develop a specific vehicle sub-system with an emphasis on the modularity, flexibility and user-friendly interface. In addition, it suits the application of control systems and automatic optimization.

Sprung Mass Dynamics

The vehicle mathematical formulation embodies five masses; the vehicle sprung or body mass and four unsprung masses, which represent the assemblies of wheels, axles, and suspensions as shown in Figs. 1-a, b. The vehicle rigid body has six DOF, which includes three translations and three rotations. Based on Newton-Euler formulation, the equations of motion of the sprung mass can be written as follow [24]:

$$\Sigma F_x = m_t \cdot \left(\dot{U} - V \cdot r + W \cdot q\right) - m_s \cdot \left[x_G \cdot \left(q^2 + r^2\right) - y_G \cdot \left(p \cdot q - \dot{r}\right) - z_G \cdot \left(p \cdot r + \dot{q}\right)\right] \quad (1)$$

$$\Sigma F_y = m_t \cdot \left(\dot{V} - W \cdot p + U \cdot r\right) - m_s \cdot \left[y_G \cdot \left(r^2 + p^2\right) - z_G \cdot \left(q \cdot r - \dot{p}\right) - x_G \cdot \left(p \cdot q + \dot{r}\right)\right] \quad (2)$$

$$\Sigma F_z = m_s \cdot \left(\dot{W} - U \cdot q + V \cdot p\right) - m_s \cdot \left[z_G \cdot \left(p^2 + q^2\right) - x_G \cdot \left(p \cdot r - \dot{q}\right) - y_G \cdot \left(q \cdot r + \dot{p}\right)\right] \quad (3)$$

$$\begin{aligned}\Sigma M_x = {} & I_{xx} \cdot \dot{p} - \left(I_{yy} - I_{zz}\right) \cdot q \cdot r + I_{yz} \cdot \left(r^2 - q^2\right) - I_{zx} \cdot \left(p \cdot q + \dot{r}\right) + I_{xy} \cdot \left(p \cdot r - \dot{q}\right) \\ & + m_s \cdot y_G \cdot \left(\dot{W} - U \cdot q + V \cdot p\right) - m_s \cdot z_G \cdot \left(\dot{V} - W \cdot p + U \cdot r\right)\end{aligned} \quad (4)$$

$$\begin{aligned}\Sigma M_y = {} & I_{yy} \cdot \dot{q} - \left(I_{zz} - I_{xx}\right) \cdot p \cdot r + I_{xz} \cdot \left(p^2 - r^2\right) - I_{xy} \cdot \left(q \cdot r + \dot{p}\right) + I_{yz} \cdot \left(q \cdot p - \dot{r}\right) \\ & + m_s \cdot z_G \cdot \left(\dot{U} - V \cdot r + W \cdot q\right) - m_s \cdot x_G \cdot \left(\dot{W} - U \cdot q + V \cdot p\right)\end{aligned} \quad (5)$$

$$\begin{aligned}\Sigma M_z = {} & I_{zz} \cdot \dot{r} - \left(I_{xx} - I_{yy}\right) \cdot p \cdot q + I_{xy} \cdot \left(q^2 - p^2\right) - I_{yz} \cdot \left(r \cdot p + \dot{q}\right) + I_{zx} \cdot \left(r \cdot q - \dot{p}\right) \\ & + m_s \cdot x_G \cdot \left(\dot{V} - W \cdot p + U \cdot r\right) - m_s \cdot y_G \cdot \left(\dot{U} - V \cdot r + W \cdot q\right)\end{aligned} \quad (6)$$

$\left(\Sigma F_x\right)$ is the net force, acting on the vehicle body in the longitudinal direction. This results from the tire forces $\left(\Sigma F_{xi}\right)$ when applying driving or braking torques at the wheels, transformed from the wheel coordinate system to the body-fixed system. Both air resistance and grade resistance due to the uneven roads are also taken into account. $\left(\Sigma F_y\right)$ is the net lateral force, expressed as a projection of the net tire forces on the vehicle y-axis. $\left(\Sigma F_z\right)$ is the net force, affecting the vehicle body in the vertical direction. The effect of inclined road surfaces is taken into consideration. $\left(\Sigma M_x, \Sigma M_y, \Sigma M_z\right)$ are the external moments of the aforementioned forces about vehicle coordinates. According to SAE Recommended Practice J670e, six coordinates systems are considered namely, earth-fixed axis system, vehicle axis system and wheel axis system at each wheel.

Unsprung Mass Dynamics

The wheels are connected to the vehicle body via springs and dampers. It is assumed that each wheel has 2-DOF, one for the vertical displacement , and the other for wheel rotation as shown in Fig. 1-d. For vertical dynamics, suspension forces are calculated based on the spring stiffness , the shock absorber damping coefficient and the vertical displacement and velocity difference between the sprung mass body corner and the wheel center. The equation of motion for unsprung masses can be written as follow:

$$m_{w_i} \cdot \ddot{z}_{w_i} = m_{w_i} \cdot g + \underbrace{C_i \cdot \left(\dot{z}_{b_i} - \dot{z}_{w_i}\right) + K_i \cdot \left(z_{b_i} - z_{w_i}\right)}_{\text{Suspension Force } (F_{si})} + F_{z_i}(z) \tag{7}$$

Drivetrain Dynamics

Considering the wheel torque balance shown in Fig. 1-c and using Newton's second law for rotational dynamics, the differential equation for the spin degree-of-freedom can be obtained as follows:

$$I_{w_i} \cdot \dot{\omega}_i = M_{Di} - M_{Ui} - M_{Bi} - \left(F_{xi} \cdot r_{di}\right) \tag{8}$$

Tire Forces and Moments

In order to reflect the real dynamics of tire, a precise tire model should be adopted in handling stability control. The Magic Formula MF provides a precise tire dynamics in both linear and nonlinear region of tire [25], the common form of MF can be expressed as follows:

$$y = D \cdot \sin\left[C \cdot \arctan\left(B \cdot x - E\left(Bx - \arctan Bx\right)\right)\right] \tag{9}$$

$$Y(X) = y(x) + S_v \qquad and \qquad x = X + S_h \tag{10}$$

Where Y represents the longitudinal force, the lateral force, or the aligning torque, and X is the longitudinal slip ratio. The tire forces in longitudinal and lateral direction are calculated based on wheel longitudinal slip (λ) and slip angle (α), as follows:

$$\lambda = \frac{V_{rw} - V_{xw}}{V_{xw}} \qquad and \qquad \alpha = \frac{V_{yw}}{V_{xw}} \tag{11}$$

Where (V_{rw}) is the product of wheel angular rotation speed and the wheel effective radius is (R_e), (V_{xw}, V_{yw}) are the longitudinal and lateral speeds at the wheel center point. (B) is the stiffness factor, which is related with the initial slope; (C) is the shape factor deciding the integral shape of the tire–force curve; (D) is the peak value; (E) is the curvature factor, which controls the curvature at the peak and the horizontal position of the peak. (S_h, S_v) are the offsets of the tire force. The experiment tire force data could be used in the fitting method to get the tire coefficients (B ,C ,D ,E) in Equation (9). The method might be defined as follows:

$$\left.\begin{aligned} C &= b_0 \\ D &= b_1 \cdot F_z^{\,2} + b_2 \cdot F_z \\ B &= \frac{\left(b_3 \cdot F_z^{\,2} + b_4 \cdot F_z\right) \cdot e^{-b_5 \cdot F_z}}{C \cdot D} \\ E &= b_6 \cdot F_z^{\,2} + b_7 \cdot F_z + b_8 \end{aligned}\right\} \tag{12}$$

$$\left.\begin{aligned} C &= a_0 \\ D &= a_1 \cdot F_z^{\,2} + a_2 \cdot F_z \\ B &= \frac{a_3 \sin\left(2\arctan\left(\frac{F_z}{a_4}\right)\theta\right)\left(1 - a_5|\gamma|\right)}{CD} \\ E &= a_6 \cdot F_z^{\,2} + a_7 \cdot F_z + a_8 \end{aligned}\right\} \tag{13}$$

The coefficients a_i (i = 0, ... ,8), b_i (i = 0, ... ,8) can be calibrated through tire force tests. In this paper, the parameters B ,C , D and E are shown in Table 1, which can be used to obtain the tire force under the nominal vertical load F_z on a certain road.

Table 1. Fitting Coefficients of the Basic Value under Nominal Conditions.

	B	C	D	E
Basic values for F_y	9.65	1.3	3690	-1.87
Basic values for F_x	11.45	1.62	4243	0.48

However when the vehicle is steering, the vertical load will transfer among four wheels, and affects the longitudinal and lateral tire forces heavily as shown in Equation (14).

$$\left.\begin{aligned} F_{z1} &= \frac{b}{2L} m_t \cdot g - \frac{h_g}{2L} m_t \cdot a_x - \frac{bh_g}{2LC} m_t \cdot a_y \\ F_{z2} &= \frac{b}{2L} m_t \cdot g - \frac{h_g}{2L} m_t \cdot a_x + \frac{bh_g}{2LC} m_t \cdot a_y \\ F_{z3} &= \frac{a}{2L} m_t \cdot g + \frac{h_g}{2L} m_t \cdot a_x + \frac{ah_g}{2LC} m_t \cdot a_y \\ F_{z4} &= \frac{a}{2L} m_t \cdot g + \frac{h_g}{2L} m_t \cdot a_x - \frac{ah_g}{2LC} m_t \cdot a_y \end{aligned}\right\} \tag{14}$$

where a_x ,a_y are the longitudinal and lateral acceleration of the vehicle body.

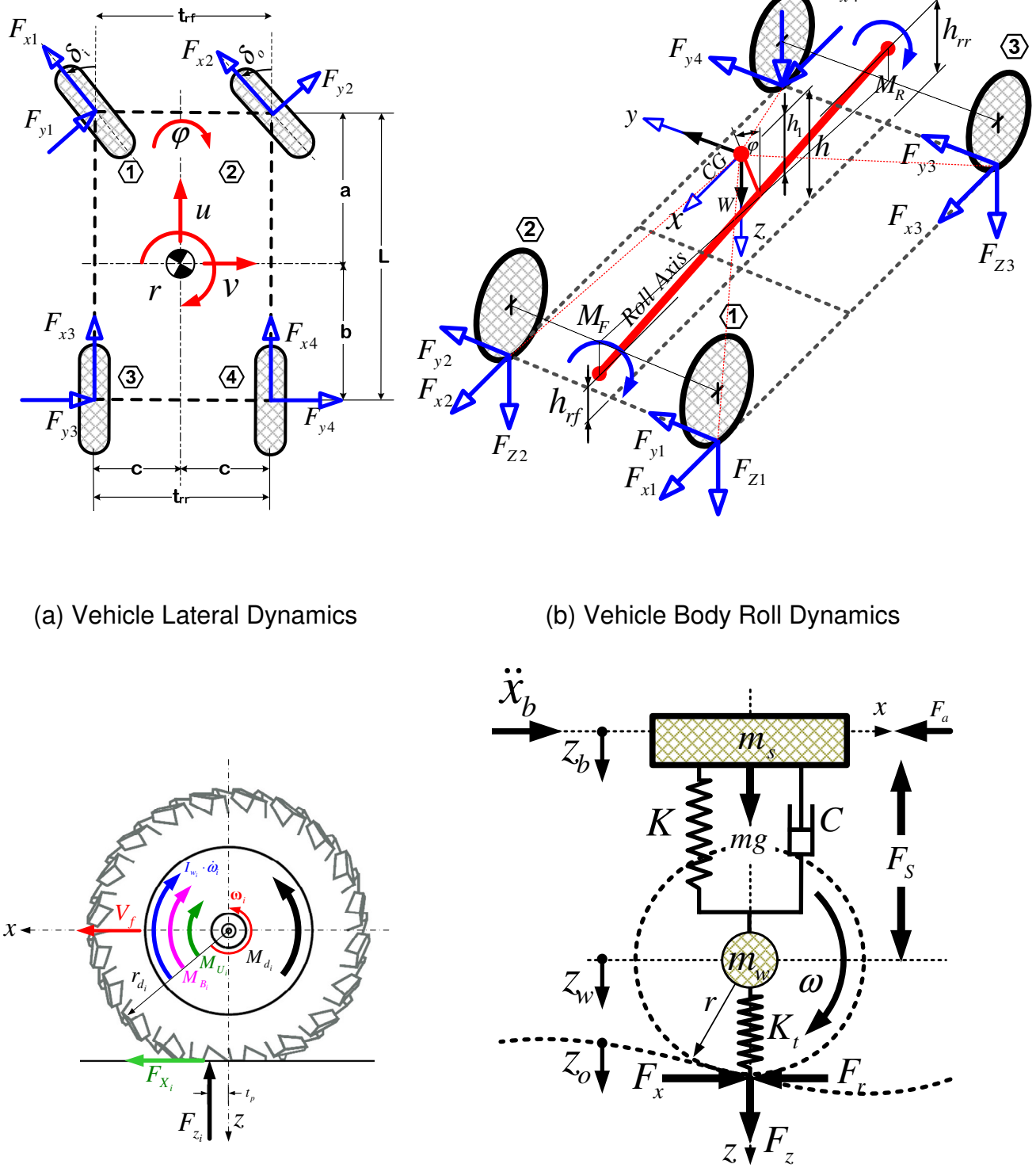

Fig. 1. 14-DOF Full Vehicle Mathematical Model Dynamics [23].

CONTROLLER DESIGN

To improve the vehicle safety in terms of handling, stability, and rollover prevention, the yaw rate (r), the sideslip angle (β), and the roll angle of the vehicle (ϕ) are controlled to follow their desired values. A reference model with 3-DOF yaw-roll plane vehicle model is adopted to calculate the desired yaw, sideslip, and roll angle. The proposed control system in this study is shown in Fig.2. The block labelled '*reference model*' generates the reference of the yaw rate, the side-slip angle, the roll angle to the driver's steering wheel angle and the input forward speed [26].

$$r_{des} = \frac{U \cdot \delta}{\left(L + \frac{M_t \cdot U^2 \cdot \left(b \cdot c_{\alpha r} - a \cdot c_{\alpha f} \right)}{2 \cdot c_{\alpha f} \cdot c_{\alpha r} \cdot L} \right)} \tag{15}$$

The desired sideslip angle and the roll angle of vehicle are assumed to be zero. There are two controllers namely the yaw moment controller which takes two inputs and one output as follow:

$$\left.\begin{aligned} &\textit{The Yaw Rate Error} \quad : e(r) = r - r_{des} \\ &\textit{The Side Slip Angle Error} : e(\beta) = \beta - \beta_{des} \\ &\textit{The Controller Outpu} \quad : M_{yaw} \end{aligned}\right\} \tag{16}$$

The roll moment controller is divided into two controllers namely feedforward and feedback controller. Four inputs of the controller are considered namely; steering wheel angle (δ), vehicle forward speed (U), roll angle error $e(\phi)$, and roll angle error rate. The output of the controller is the roll moment (M_ϕ).

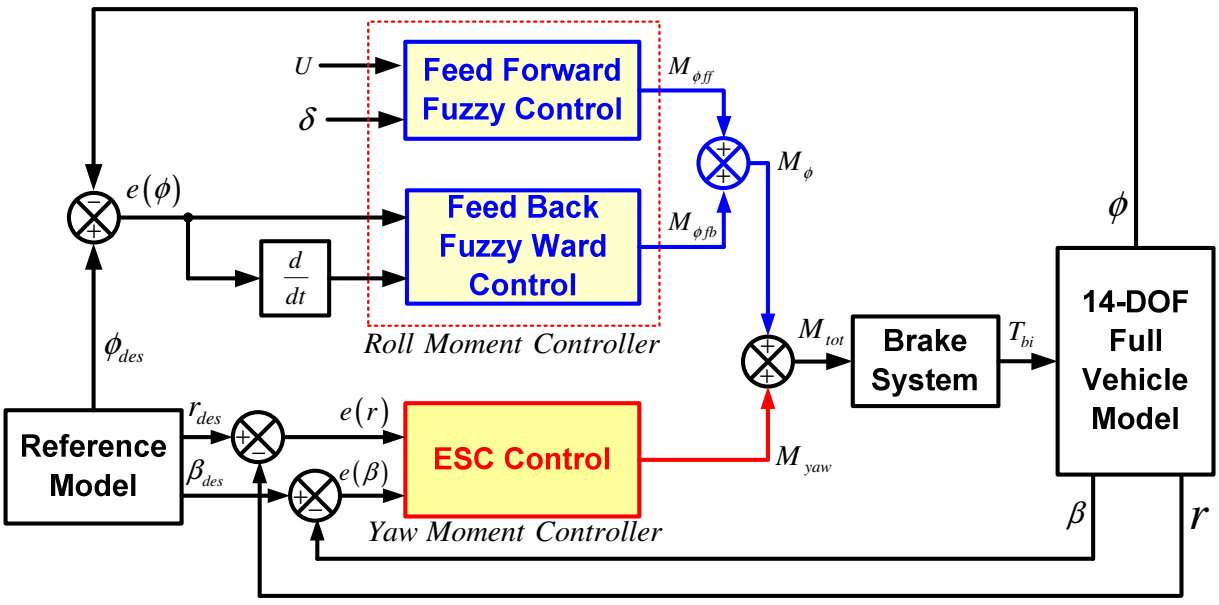

Fig. 2. Block Diagram of the Integrated Controller.

Yaw Moment Controller

Yaw moment controller calculates the counter direct yaw moment based on the side slip angle error and the yaw rate error. As illustrated in Fig. 3, five membership functions are selected to represent the side slip angle error, and the yaw rate error which are two trapezoidal and three triangle membership functions. On the other hand eleven membership functions are selected to represent the counter yaw moment as an output of the controller which is two trapezoidal and nine triangle membership functions. The five variables necessary to calculate both the side slip angle error and the yaw rate error are negative big (NB), negative small (NS), zero (ZO), positive small (PS) and positive big (PB). The eleven variables for the counter yaw moment are (N5, N4, N3, N2, N1, ZO, P1, P2, P3, P4, and P5). The universe of discourse for the inputs was set based on their operating range. The direct yaw moment from fuzzy control is obtained with a scaling factor. The rule base of the ESP Fuzzy controller is given in Table 2.

Table 2. Fuzzy Logic Rule Base for Active Yaw Controller.

Slip angle error/yaw rate error	NB	NS	ZO	PS	PB
NB	N1	N1	ZO	P1	P1
NS	N2	N2	ZO	P2	P2
ZO	N3	N3	ZO	P3	P3
PS	N4	N4	ZO	P4	P4
PB	N5	N5	ZO	P5	P5

Active Roll Controller

The proposed active roll control strategy consists of feedback fuzzy logic control and feedforward fuzzy logic control as presented in Fig.2. For the feedforward fuzzy logic control, road steering wheel angle and the longitudinal vehicle velocity are chosen as the inputs and the counter roll moment is selected as the output. The inputs for the feedback fuzzy logic control were the roll angle error and its error rate and the output is the counter roll moment. The roll angle error is defined as the difference between the desired roll angle (ϕ_{des}) and actual roll angle (ϕ). The resultant counter roll (M_{ϕ}) which the summation of ($M_{\phi ff}$) the counter roll moment due to the feedforward fuzzy control, and ($M_{\phi fb}$) the counter roll moment due to the feedback fuzzy control.

Feed forward fuzzy control calculates the counter roll moment based on the road wheel steering angle and longitudinal vehicle velocity as presented in Fig. 4, seven Gaussian membership functions were selected for road steering wheel angle, five Gaussian membership functions for the longitudinal vehicle velocity error rate and seven Gaussian memberships functions for the counter roll moment. The Gaussian membership function was used due to their smooth mapping property. The seven variables for the road steering input and counter roll moment are negative large (NL), negative medium (NM), negative small (NS), zero (Z), positive small (PS), positive medium (PM), and positive large (PL). The five variables for the longitudinal vehicle velocity are very slow (VS), slow (S), normal (N), fast (F), and very fast (VF), Table 3. The universe of discourse for the inputs was set based on their operating range.

Feedback fuzzy control, each roll angle error, roll angle error rate and counter roll moment has five Gaussian membership functions. The five variables for the roll angle error, roll angle error rate and counter roll moment are negative medium (NM), negative small (NS), zero (Z), positive small (PS), and positive medium (PM), see Table 4. The membership functions for roll angle error roll angle error rate, and counter roll moment are depicted in Fig. 5. The universe of discourse for the counter roll moment was normalized in the range [-1 1]. Fuzzy control is a non-linear control method and can be used to deal with complicated non-linear dynamic control problems. The main advantage of fuzzy models in comparison with conventional mathematical models is the possibility of elaborating them on the basis of far lesser amounts of information about a system.

Table 3. Rule Base for Feedforward Fuzzy Logic Controller.

Speed/steering	NL	NM	NS	Z	PS	PM	PL
VS	Z	Z	Z	Z	Z	Z	Z
S	NM	NM	NM	Z	PM	PM	PM
N	NL	NM	NM	Z	PM	PM	PL
F	NL	NL	NL	Z	PL	PL	PL
VF	NL	NL	NL	Z	PL	PL	PL

Table 4. Rule Base for Feedback Fuzzy Logic Controller.

Roll error/roll error rate	NM	NS	Z	PS	PM
NM	NM	NM	NM	PM	PM
NS	NM	NS	NS	PS	PM
Z	NM	NS	Z	PS	PM
PS	NM	NS	PS	PS	PM
PM	NM	NM	PM	PM	PM

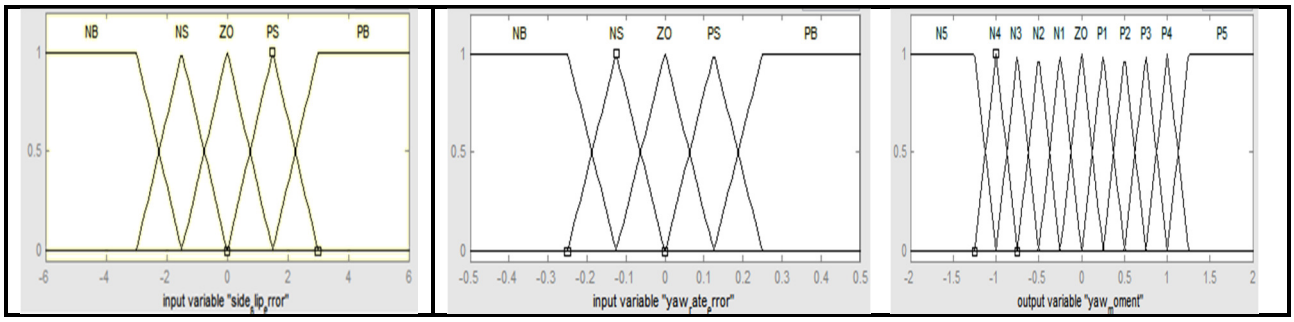

Fig. 3. Memberships Function of the Yaw Moment Controller.

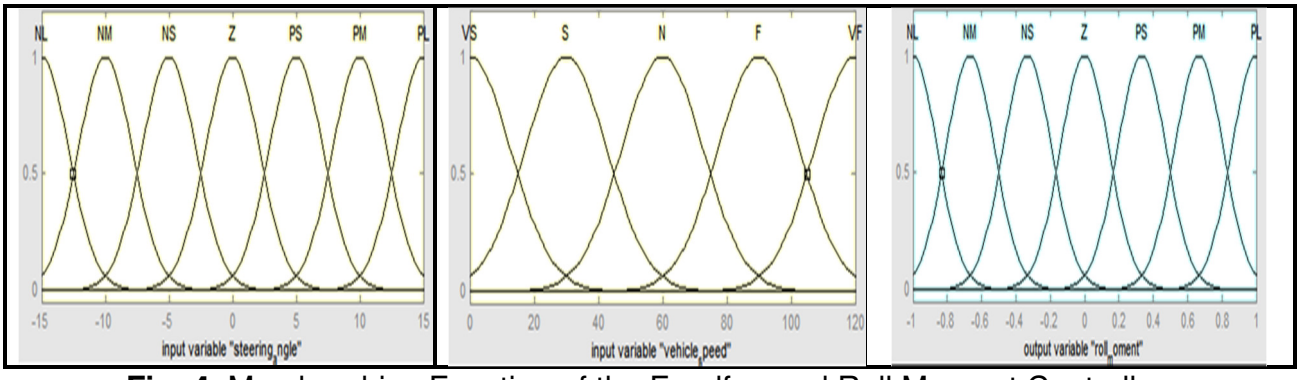

Fig. 4. Memberships Function of the Feedforward Roll Moment Controller.

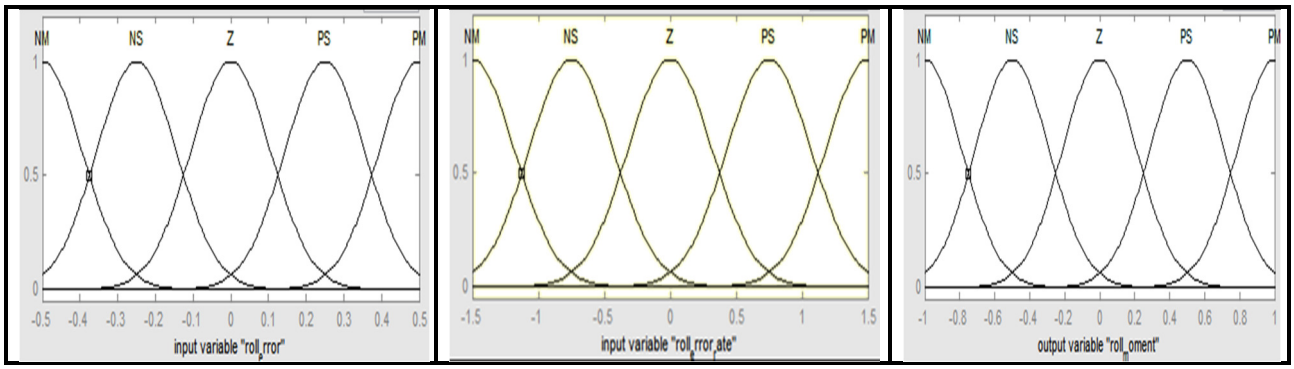

Fig. 5. Memberships Function of the Feedback Ward Roll Moment Controller.

MODEL SIMULATION

A simulation study is conducted to show the effectiveness of the proposed controller. Simulation is done using full vehicle model and simulation software based on MATLAB and SIMULINK. The parameters characterizing of the vehicle model are shown in Appendix A. These parameters are corresponding to a typical vehicle model. The fuzzy logic controller was designed using MATLAB's fuzzy logic toolbox. To clarify the effects of the proposed controller, vehicle dynamics both with and without the controller are shown. Simulation runs are made for all wheel drive vehicle. The effectiveness of the controller is shown considering four different standard cornering test maneuvers at different vehicle speeds namely: lane change maneuver, J turn maneuver, fishhook maneuver, and double lane change maneuvers.

RESULTS AND DISCUSSION

Using continuous time simulation, the simulation results are performed for a four different maneuvers inputs namely, lane change, J turn, fishhook, and double lane change at a vehicle forward velocity of 20 and 30 m/s respectively with a nominal road friction coefficient of μ= 0.9, a value deemed to be generally representative of dry pavement.

The response of uncontrolled, based yaw-sideslip only, based roll only, and integrated control are shown for four stability indices performance which are lateral acceleration, roll angle, side slip angle, and yaw rate with forward vehicle velocity of 20 and 30 m/s respectively. In both cases, without a controller the vehicle stability indices performance is too large and oscillates.

Lane change maneuver is often needed to avoid obstacles in real-life situations, and it is a very useful to evaluate both the stability and handling of a vehicle as shown in Figs 6-7. The based yaw-sideslip only, based roll only, and integrated controllers all keep lateral acceleration, roll angle, side slip angle, and yaw rate in the desired region and have fast rise times. However, the integrated control shows the best results. The root mean square values of the uncontrolled system, active based yaw-sideslip control, active based roll control, and active integrated control for lane change maneuver at 30 m/s are tabulated in Table 5.

Table 5. RMS for Lane Change Steer Test at Vehicle Speed 30 m/s.

Criteria	Uncontrolled	Based yaw-side slip	Based roll	Integrated
Lateral acceleration (m/s^2)	2.344	1.696	1.927	1.3406
Side slip angle (deg)	1.086	0.522	0.6793	0.3436
Yaw rate (deg/sec)	5.914	4.0737	4.7027	3.2070
Roll angle (deg)	1.465	1.0467	1.1974	0.8262

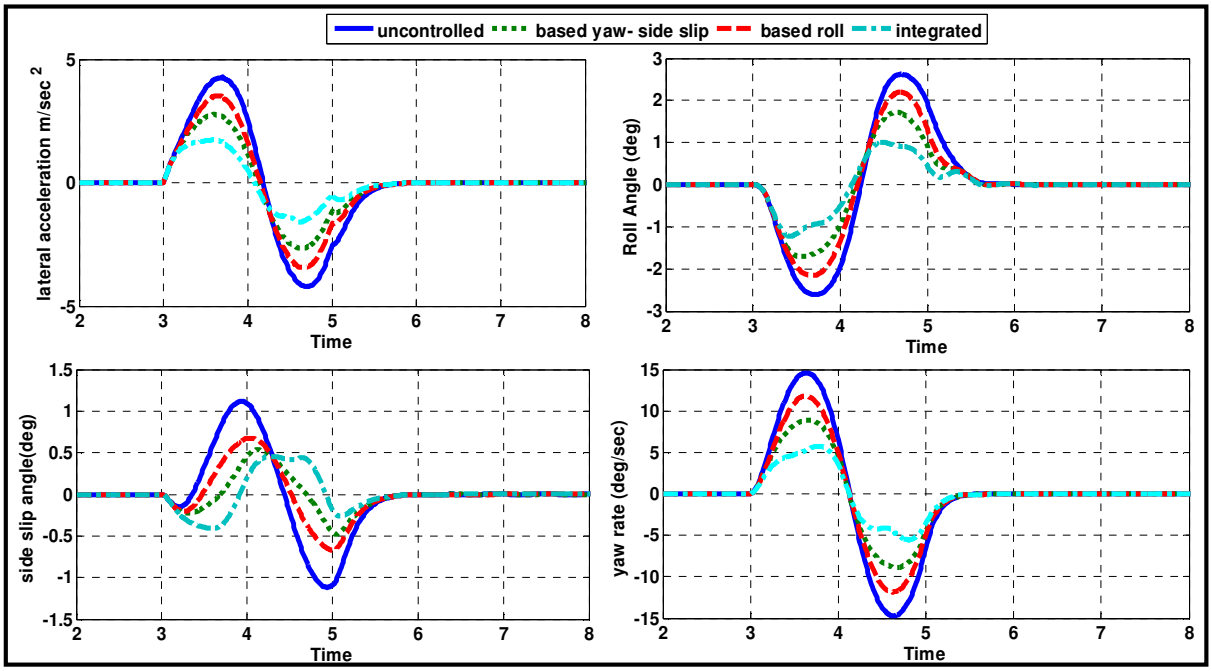

Fig. 6. Vehicle Response during Lane Change with Vehicle Speed 20 m/s.

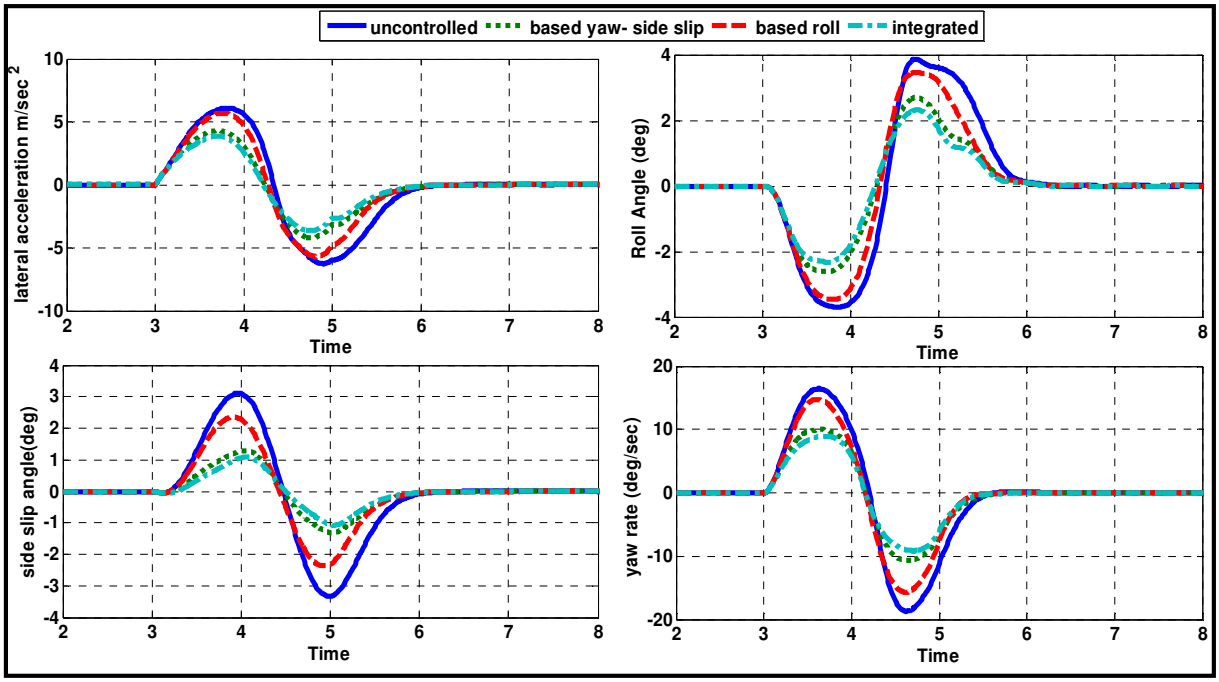

Fig. 7. Vehicle Response during Lane Change with Vehicle Speed 30 m/s.

Figs 8-9 show the vehicle response for uncontrolled, based yaw-sideslip only, based roll only, and integrated control during J-turn maneuver with maximum angle of 90 degree at speeds 20 and 30 m/s respectively.

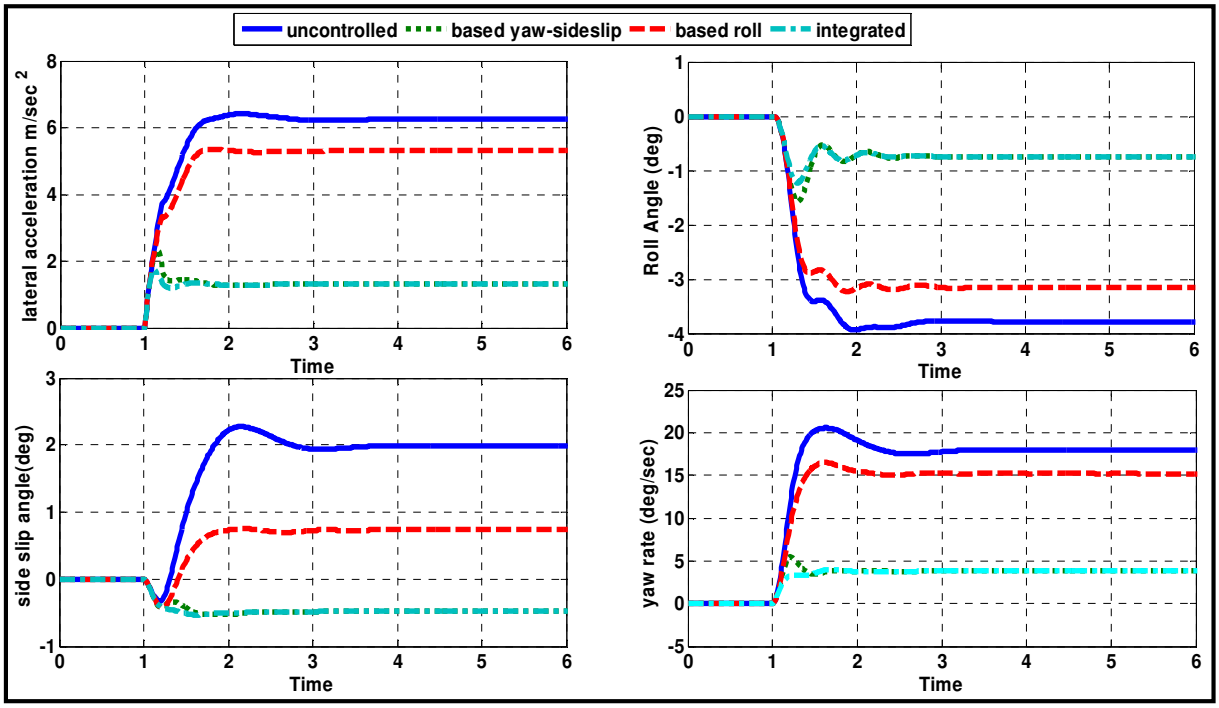

Fig. 8. Vehicle Response during J-T with Vehicle Speed 20 m/s.

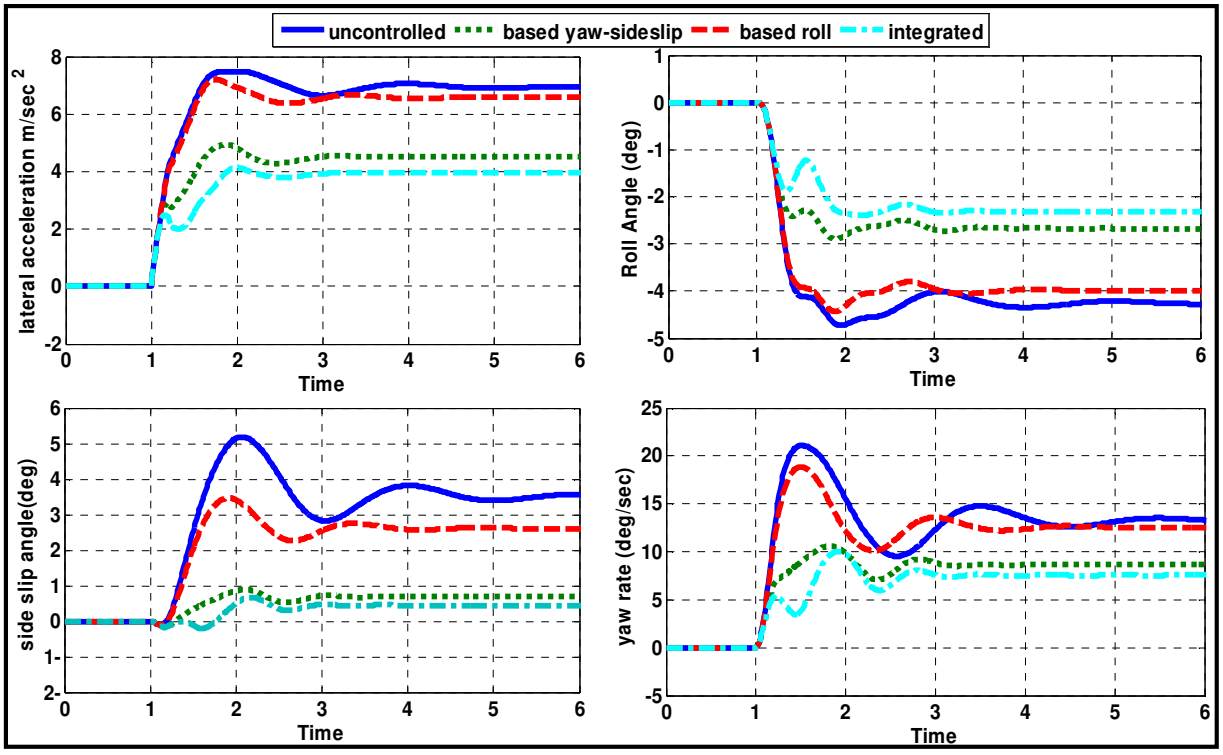

Fig. 9. Vehicle Response during J- Turn with Vehicle Speed 30 m/s.

Based on the simulation results, stability indices performance are greatly improved with the integrated and based yaw-sideslip only control. The root mean square values of the uncontrolled system, active based yaw-sideslip control, active based roll control, and active integrated control for J turn maneuver at 30 m/s are tabulated as shown in Table 6.

Table 6. RMS for J Turn Steer Test at Vehicle Speed 30 m/s.

Criteria	Uncontrolled	Based yaw-side slip	Based roll	Integrated
Lateral acceleration (m/s^2)	6.499	5.0276	5.9609	3.7584
Side slip angle (deg)	3.358	1.0477	2.0057	0.4474
Yaw rate (deg/sec)	12.919	9.7523	11.6639	7.2671
Roll angle (deg)	3.983	2.9922	3.5958	2.1984

To demonstrate the effect of based yaw-sideslip only, based roll only, and integrated controllers in preventing rollovers. The simulation is performed with steering input fishhook maneuver with maximum angle of 140 degree at speed 20 and 30 m/s respectively. The simulation results are depicted in Figs 10-11, which are reflecting a remarkable improvement in both vehicle handling and stability.

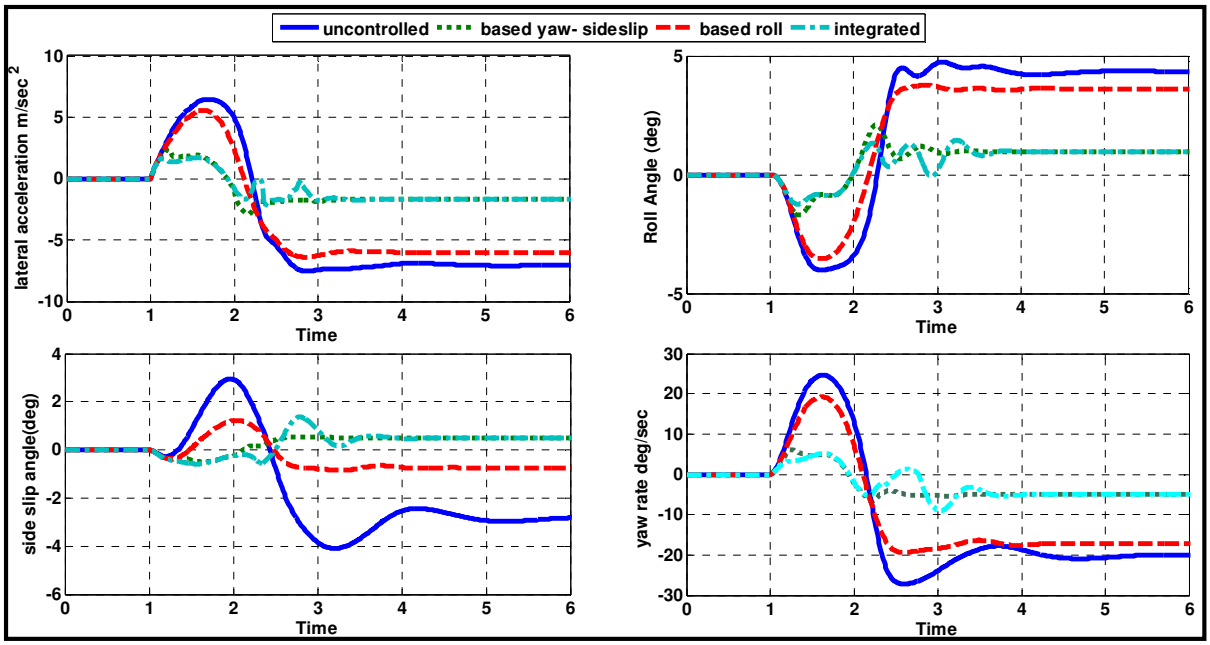

Fig. 10. Vehicle Response during Fishhook Turn with Vehicle Speed 20 m/s.

The root mean square values of the uncontrolled system, active based yaw-sideslip control, active based roll control, and active integrated control for fishhook turn maneuver at 30 m/s are tabulated in Table 7.

Table 7. RMS for Fishhook Steer Test at 30 m/s.

Criteria	Uncontrolled	Based yaw-side slip	Based roll	Integrated
Lateral acceleration (m/s^2)	6.6708	4.4599	6.134	1.7206
Side slip angle (deg)	1.086	0.7434	0.8654	0.2507
Yaw rate (deg/s)	15.5319	8.9045	12.5592	3.2463
Roll angle (deg)	4.1553	2.6578	3.7542	0.9913

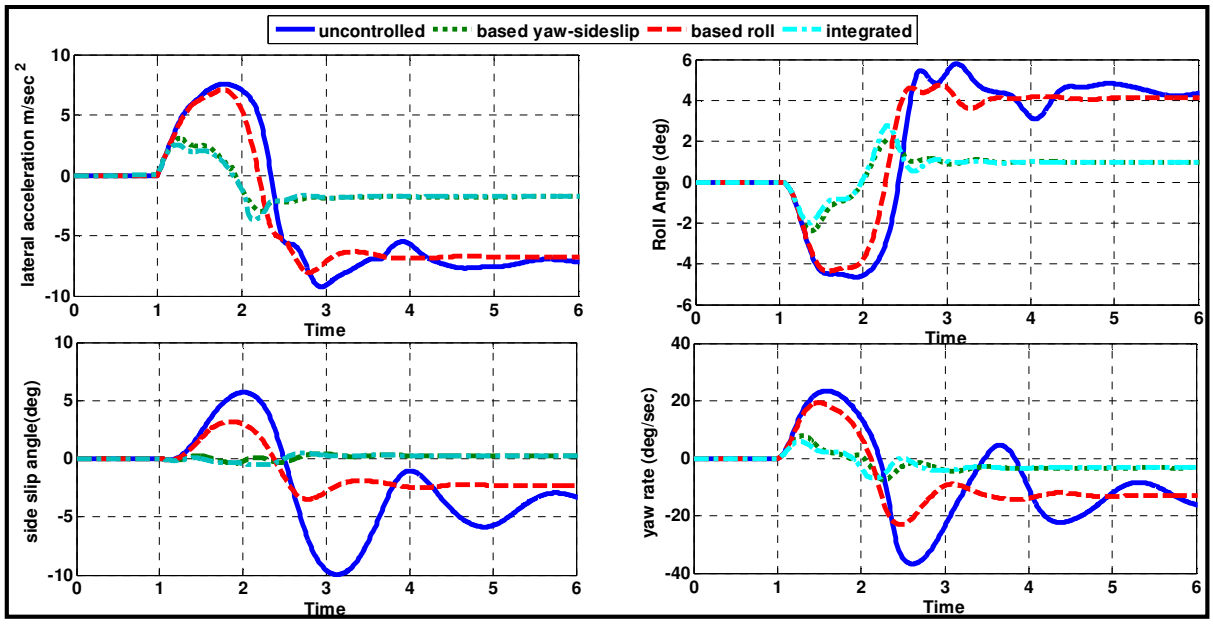

Fig. 11. Vehicle Response during Fishhook Turn with Vehicle Speed 30 m/s.

A double lane-change maneuver is a typical driving condition and commonly used to estimate vehicle handling performance. Their lateral acceleration, sideslip angle, roll angle and yaw rate responses on a double lane-change road at speed 20 and 30 m/s respectively are compared as shown in Figs 12-13.

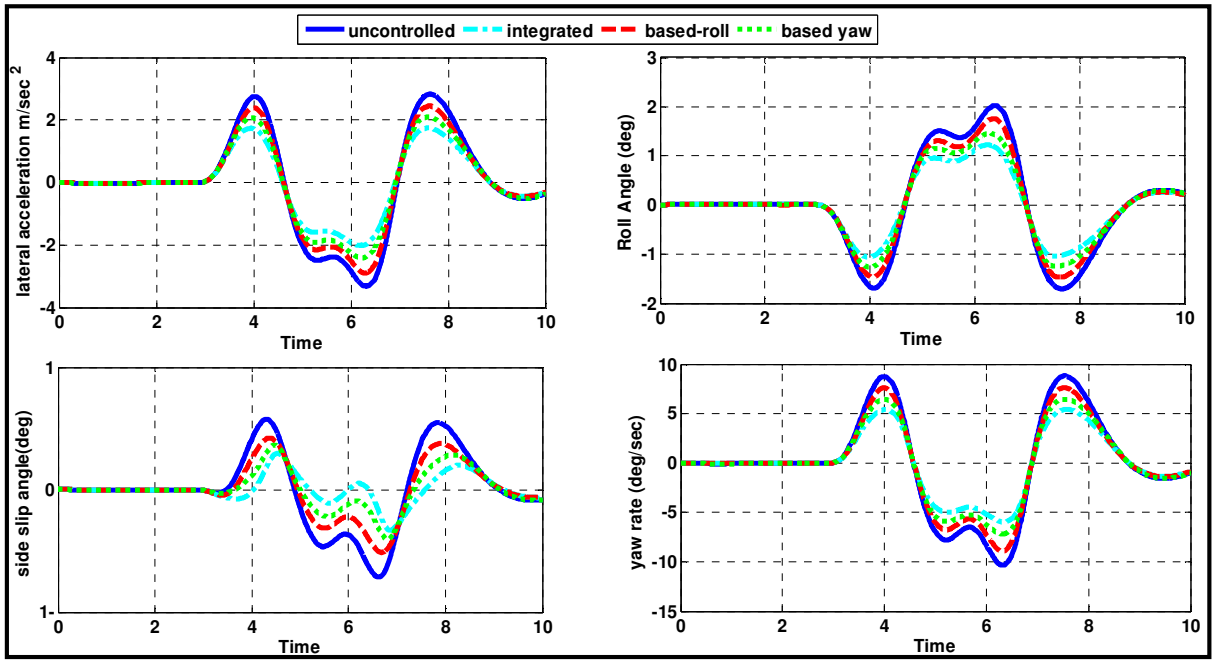

Fig. 12. Vehicle Response during Double Lane Change with Vehicle Speed 20 m/s.

The root mean square values of the uncontrolled system, active based yaw-sideslip control, active based roll control, and active integrated control for double lane change maneuver at 30 m/s are listed in Table 8.

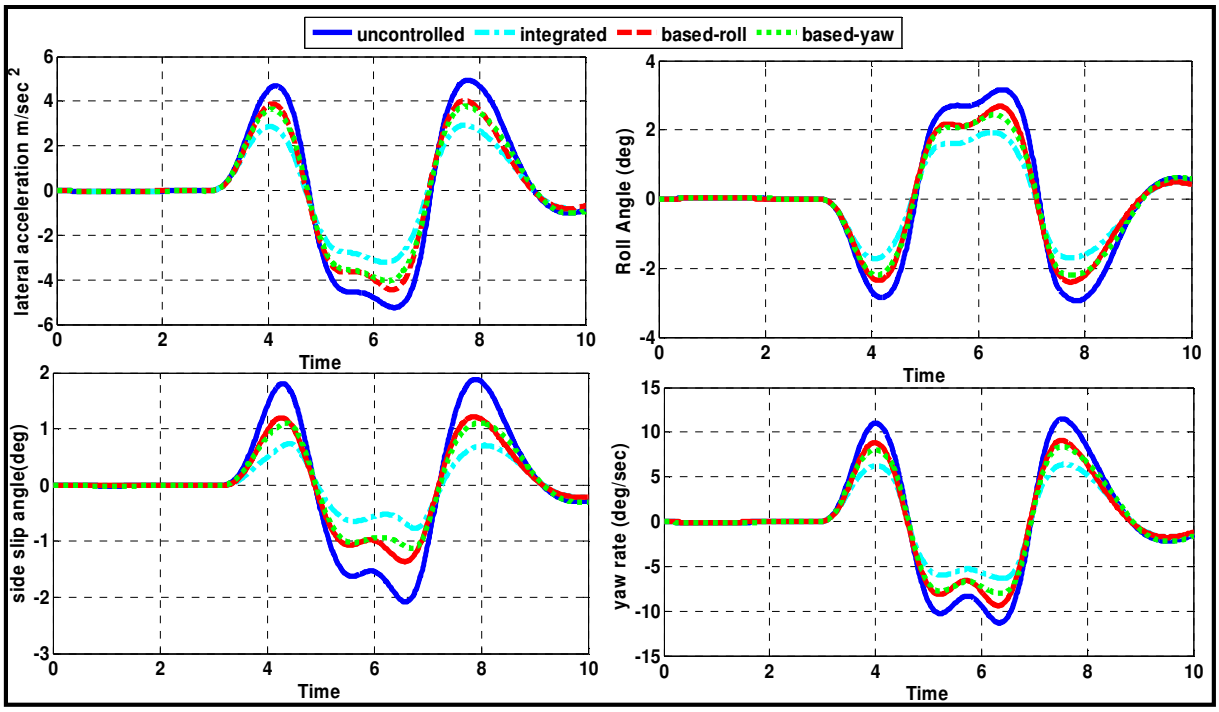

Fig. 13. Vehicle Response during Double Lane Change with Vehicle Speed 30 m/s.

Table 8. RMS for Double Lane Change Steer Test at Vehicle Speed 30 m/s.

Criteria	Uncontrolled	Based yaw-side slip	Based roll	Integrated
Lateral acceleration (m/s^2)	2.839	2.3277	2.3852	1.9314
Side slip angle (deg)	1.0217	0.6936	0.7249	0.4891
Yaw rate (deg/s)	6.1177	4.9660	5.0909	4.1099
Roll angle (deg)	1.7191	1.3989	1.4370	1.1578

The above simulation results show that a vehicle equipped with the ESP control system can sustain its handling and stability in various hazardous conditions (different maneuvers) compared to the uncontrolled vehicle. In addition, the ESP system can improve the vehicle response in respect to the driver's experience to ensure safety. Finally, according to the simulation results, the integrated control give the best result compared to the other controllers, while the based yaw-sideslip control appear the significate results. In comparison to the well published literature for example in [11], the obtained results of the proposed controller are matched both in the qualitative and quantitative manner.

CONCLUSIONS

The current paper proposed an integrated control system that integrates the active yaw control and active roll control with three fuzzy logic based controller to improve the vehicle handling, stability, and rollover prevention. The proposed system generates differential braking for this purpose using yaw rate error, side slip angle error, and roll angle as inputs.

The performance of the proposed system has been evaluated through numerical simulation of the mathematical model of a vehicle using MATLAB/Simulink. The fuzzy logic method based controller is shown to be an effective means of controlling vehicle handling and stability. The simulation results show that a vehicle with the proposed integrated control system has smaller yaw rate, side slip angle, roll angle, and lateral acceleration than an uncontrolled vehicle for lane change, J turn, fishhook, and double lane change steer inputs with two different vehicle speeds.

REFERENCES

[1] A. T. Van Zanten, R. Erhardt, and G. Pfaff, "VDC, the vehicle dynamics control system of Bosch," SAE Technical Paper, 1995.

[2] A. T. Van Zanten, "Bosch ESP systems: 5 years of experience," SAE Technical Paper, 2000.

[3] A. Sorniotti, and M. Velardocchia, "Hardware-in-the-loop (HIL) testing of ESP (electronic stability program) commercial hydraulic units and implementation of new control strategies," SAE Technical Paper 0148-7191, 2004.

[4] N. Hamzah, Y. M. Sam, H. Selamat, M. K. Aripin, and M. F. Ismail, "Vehicle stability enhancement based on second order sliding mode control," in Control System, Computing and Engineering (ICCSCE), IEEE International Conference on, pp. 580-585, 2012

[5] D. Yin and J.-S. Hu, "Active approach to Electronic Stability Control for front-wheel drive in-wheel motor electric vehicles," International Journal of Automotive Technology, vol. 15, pp. 979-987, 2014.

[6] L. Palkovics, Á. Semsey, and E. Gerum, "Roll-over prevention system for commercial vehicles–additional sensorless function of the electronic brake system," Vehicle System Dynamics, vol. 32, pp. 285-297, 1999.

[7] B.-C. Chen and H. Peng, "Differential-braking-based rollover prevention for sport utility vehicles with human-in-the-loop evaluations," Vehicle System Dynamics, vol. 36, pp. 359-389, 2001.

[8] S. Solmaz, M. Corless, and R. Shorten, "A methodology for the design of robust rollover prevention controllers for automotive vehicles: Part 1-Differential Braking," in Decision and Control, 45th IEEE Conference, pp. 1739-1744, 2006.

[9] J. Yoon and K. Yi, "A rollover mitigation control scheme based on rollover index," in American Control Conference, 2006.

[10] S. B. Choi, "Practical vehicle rollover avoidance control using energy method," Vehicle System Dynamics, vol. 46, pp. 323-337, 2008.

[11] J. Cao, L. Jing, K. Guo, and F. Yu, "Study on Integrated Control of Vehicle Yaw and Rollover Stability Using Nonlinear Prediction Model," Mathematical Problems in Engineering, vol. 2013, 2013.

[12] M. B. Alberding, J. Tjønnås, and T. A. Johansen, "Integration of vehicle yaw stabilisation and rollover prevention through nonlinear hierarchical control allocation," Vehicle System Dynamics, vol. 52, pp. 1607-1621, 2014.

[13] S. Solmaz, M. Corless, and R. Shorten, "A methodology for the design of robust rollover prevention controllers for automotive vehicles: Part 2-Active Steering," in Decision and Control, 45th IEEE Conference, pp. 1739-1744, 2006.

[14] S. Yim, K. Jeon, and K. Yi, "An investigation into vehicle rollover prevention by coordinated control of active anti-roll bar and electronic stability program," International Journal of Control, Automation and Systems, vol. 10, pp. 275-287, 2012.
[15] K. Jeon, H. Hwang, S. Choi, J. Kim, K. Jang, and K. Yi, "Development of an electric active rollcontrol (ARC) algorithm for a SUV," International journal of automotive technology, vol. 13, pp. 247-253, 2012.
[16] M. Biglarbegian, W. Melek, and F. Golnaraghi, "Design of a novel fuzzy controller to enhance stability of vehicles," in Fuzzy Information Processing Society, NAFIPS'07. Annual Meeting of the North American, pp. 410-414, 2007.
[17] R. Tchamna, E. Youn, and I. Youn, "Combined control effects of brake and active suspension control on the global safety of a full-car nonlinear model," Vehicle System Dynamics, vol. 52, pp. 69-91, 2014.
[18] E. Elbeheiry, Y. Zeyada, and M. Elaraby, "Handling capabilities of vehicles in emergencies using coordinated AFS and ARMC systems," Vehicle System Dynamics, vol. 35, pp. 195-215, 2001.
[19] A. Hac, "Influence of active chassis systems on vehicle propensity to maneuver-induced rollovers," SAE Technical Paper, 2002.
[20] S. Yim, "Design of a robust controller for rollover prevention with active suspension and differential braking," Journal of mechanical science and technology, vol. 26, pp. 213-222, 2012.
[21] H. Her, J. Suh, and K. Yi, "Integrated control of the differential braking, the suspension damping force and the active roll moment for improvement in the agility and the stability," Proceedings of the Institution of Mechanical Engineers, Part D: Journal of Automobile Engineering, p. 0954407014550502, 2014.
[22] R. Rajamani and D. Piyabongkarn, "New paradigms for the integration of yaw stability and rollover prevention functions in vehicle stability control," Intelligent Transportation Systems, IEEE Transactions on, vol. 14, pp. 249-261, 2013.
[23] A. M. Sharaf 'Real-time Assessment of Vehicle Response in a Virtual Proving Ground', Int. J. Heavy Vehicle Systems, Vol. 20, No. 2, pp.174–189, 2013.
[24] H. Pacejka, Tire and vehicle dynamics: Elsevier, 2005.
[25] J. R. Ellis, Vehicle handling dynamics, 1994.
[26] R. Rajamani, Vehicle dynamics and control: Springer Science & Business Media, 2011.

APPENDIX-A

Table (A-1). Parameters of System Model.

Model Parameters	Symbol	Value	Units
Total mass of the vehicle	M_t	1840.9	Kg
Sprung mass of the vehicle	M_s	1665.50	Kg
Front unsprung mass at each wheel	M_{wf}	44.83	Kg
Rear unsprung mass at each wheel	M_{wr}	41.42	Kg
Mass moment of inertia of the sprung mass about x axis	I_{xx}	734	Kg.m^2
Mass moment of inertia of the sprung mass about y axis	I_{yy}	3983	Kg.m^2
Mass moment of inertia of the sprung mass about z axis	I_{zz}	4240	Kg.m^2
Mass product moment of inertia of the vehicle sprung mass	I_{xz}	-15.6	Kg.m^2
Mass moment of inertia of wheels	I_{wi}	1.5	Kg.m^2
Stiffness coefficient of front suspension spring	K_f	20090	N/m
Stiffness coefficient of rear suspension spring	K_r	22700	N/m
Damping coefficient of front suspension	C_f	2000	N.s/m
Damping coefficient of rear suspension	C_r	2230	N.s/m
Cornering stiffness of front, rear tyres	$C_{\alpha f}, _{\alpha r}$	60000	N/rad
Distance from CG to the front axle	a	1.4499	m
Distance from CG to the rear axle	b	1.5801	m
Wheelbase (distance between front and rear axle)	L	3.030	m
Wheel track at front and rear axle	t_{rf}, t_{rr}	1.558	m
Dynamic rolling radius of each wheel	r_{di}	0.3169	m